3D Forward and Back-Projection for X-Ray CT Using Separable Footprints with Trapezoid Functions

Yong Long and Jeffrey A. Fessler

EECS Dept.
University of Michigan

First CT Meeting
June 9, 2010

Introduction

- Iterative methods for 3D image reconstruction have the potential to improve image quality over conventional filtered back projection (FBP) based methods in X-ray CT.
- The primary computation burden of iterative methods is 3D cone-beam forward- and back-projection using system matrix ($\boldsymbol{A}'$).
- Infeasible to store $\boldsymbol{A}$ due to its huge size.
- Forward projection goal: compute $\boldsymbol{Ax}$ rapidly but accurately on the fly.
- Back projection goal: compute $\boldsymbol{A}'\boldsymbol{y}$ using exact transpose, rapidly but accurately on the fly.
- Many methods exist, all of which compromise between computational complexity and accuracy.

Separable Footprint (SF) Method

- The distance-driven (DD) is a current state-of-the-art method (De Man and Basu, PMB 2004).
- We proposed the SF-TR (trapezoid/rectangle) method (Long *et al.* Fully3D 2009, IEEE T-MI to appear).
- SF-TT (trapezoid/trapezoid) is the new extension reported here. (Inspired by reviewer inquiry.)
- Summary:
  - Quantitative accuracy: SF-TT $>$ SF-TR $>$ DD
  - Qualitative results: SF-TT $\approx$ SF-TR $>$ DD
  - Computation time: SF-TT $>$ ST-TR $\approx$ DD

Axial Cone-Beam Geometry

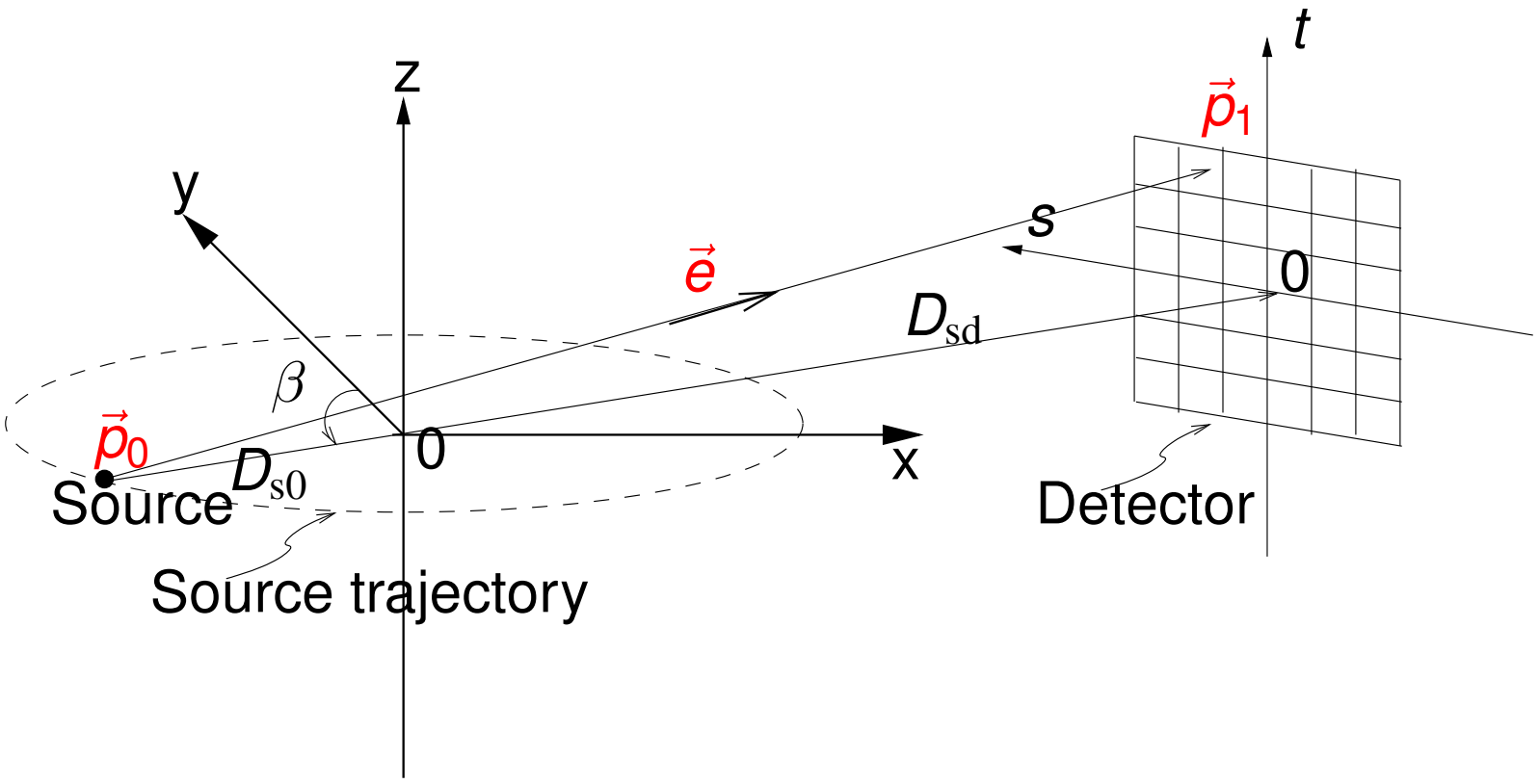

β denotes the angle of the source point counter-clockwise from the y axis.

s and t denote detector plane coordinates

Cone-Beam Projection

- Ideal cone-beam projection of a 3D object $f(\vec{x})$:

$$p(s,t;\beta) = \int_{\mathcal{L}(s,t,\beta)} f(x,y,z)\,\mathrm{d}\ell, \tag{1}$$

where ray is

$$\mathcal{L}(s,t,\beta) = \left\{ \vec{p}_0 + \alpha\vec{e} : \alpha \in \left[0, \sqrt{D_{\mathrm{sd}}^2 + s^2 + t^2}\right] \right\}, \tag{2}$$

and $\vec{e} = \vec{e}(s,t,\beta)$ is the direction vector from $\vec{p}_0$ to $\vec{p}_1$.

Detector blur model

- Shift-invariant detector blur accounts for finite detector cell size:

$$h(s,t) = \frac{1}{r_s r_t} \operatorname{rect}\left(\frac{s}{r_s}\right) \operatorname{rect}\left(\frac{t}{r_t}\right), \tag{3}$$

where r_s and r_t denote the width along s and t respectively.

- Ideal (noiseless) sampled projection views:

$$\begin{aligned} \bar{y}_\beta[s_k, t_l] &= \iint h(s_k - s, t_l - t) p(s,t;\beta) \, \mathrm{d}s \, \mathrm{d}t \\ &= \iint h(s_k - s, t_l - t) \left(\int_{\mathcal{L}(s,t,\beta)} f(x,y,z) \, \mathrm{d}\ell \right) \mathrm{d}s \, \mathrm{d}t, \end{aligned} \tag{4}$$

where $k = 0, \ldots, N_\mathrm{s} - 1$ and $l = 0, \ldots, N_\mathrm{t} - 1$.

- Discretized object based on a common basis function $\beta_0(\vec{x})$:

$$f(\vec{x}) = \sum_{\vec{n}} f[\vec{n}] \, \beta_0\left((\vec{x} - \vec{c}[\vec{n}]) \oslash \vec{\Delta} \right), \tag{5}$$

where the grid spacing is $\vec{\Delta} = (\Delta_1, \Delta_2, \Delta_3)$, and $\Delta_1 = \pm\Delta_2$ hereafter.

Cone-Beam 3D System Model (cont.)

- Substitute object model (5) into measurement model (4) $\Rightarrow$

$$\bar{y}_\beta[s_k, t_l] = \sum_{\vec{n} \in S} a_\beta[s_k, t_l; \vec{n}] f[\vec{n}]. \tag{6}$$

- System matrix $\boldsymbol{A}$ elements ("blurred footprint")

$$\begin{aligned} a_\beta[s_k, t_l; \vec{n}] &= F(s_k, t_l; \beta; \vec{n}) \\ &= \iint h(s_k - s, t_l - t) q(s, t; \beta; \vec{n}) \, \mathrm{d}s \, \mathrm{d}t \, . \end{aligned} \tag{7}$$

- Footprint of the basis function

$$q(s, t; \beta; \vec{n}) = \int_{\mathcal{L}(s,t,\beta)} \beta_0 \left((\vec{x} - \vec{c}[\vec{n}]) \oslash \vec{\Delta} \right) \mathrm{d}\ell \, . \tag{8}$$

- Forward projection methods compute (8) and (7) approximately.

Exact footprint and blurred footprint, for rectangular cuboid (voxel)

$$F(s_k, t_l; \beta; \vec{n}) = \iint h(s_k - s, t_l - t)\, q(s, t; \beta; \vec{n})\, \mathrm{d}s\, \mathrm{d}t$$

$$h(s, t) = \frac{1}{r_s r_t} \operatorname{rect}\left(\frac{s}{r_s}\right) \operatorname{rect}\left(\frac{t}{r_t}\right)$$

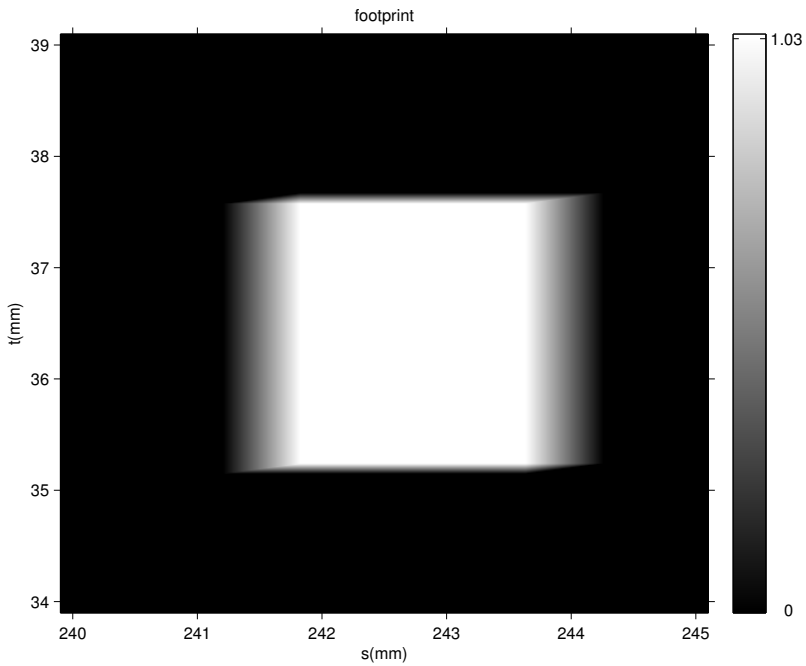

$q(s, t; \beta; \vec{n})$

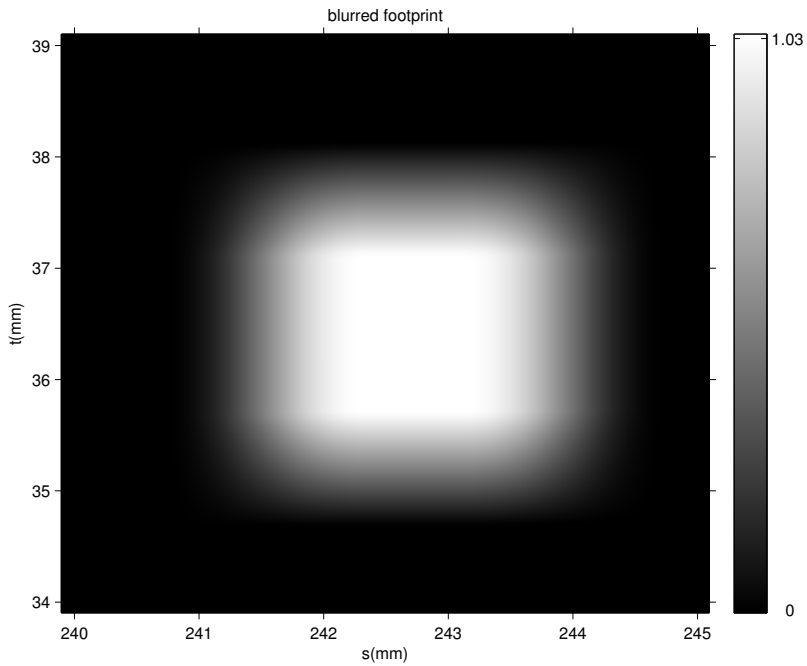

$F(s, t; \beta; \vec{n})$

Cone-Beam Projections of Voxel Basis Functions (*Footprints*)

(0, 0, 0) mm

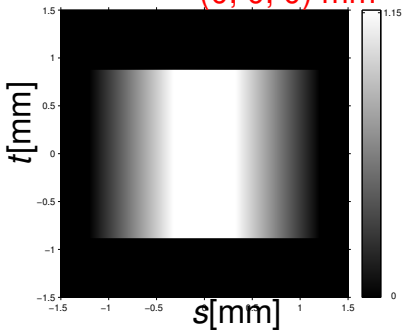

(100, 150, 15) mm

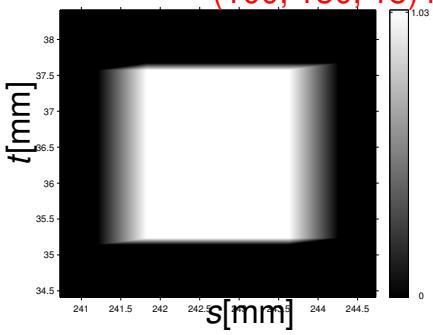

(93, 93, 93) mm

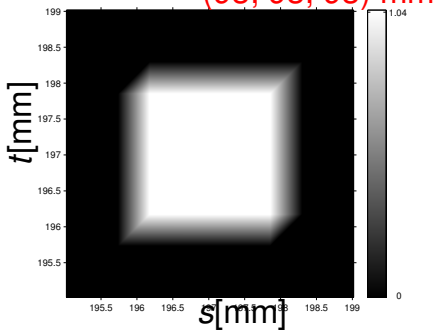

True footprints.

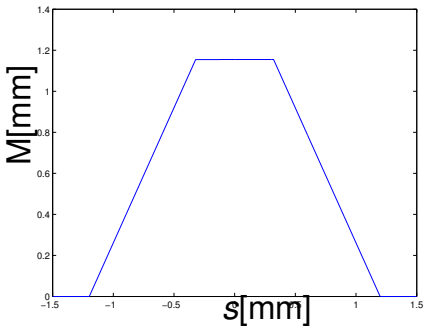

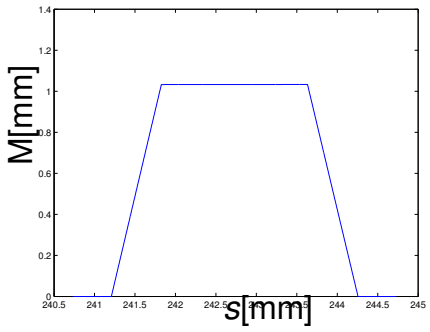

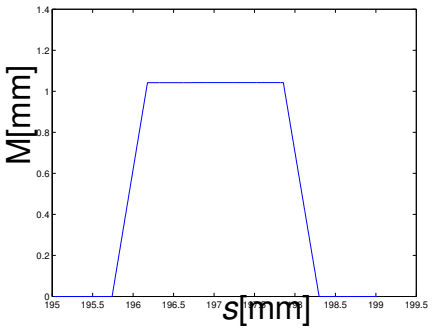

Profiles in *s*.

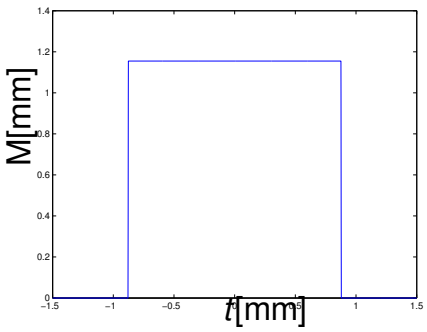

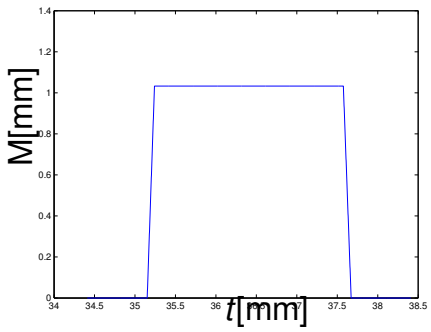

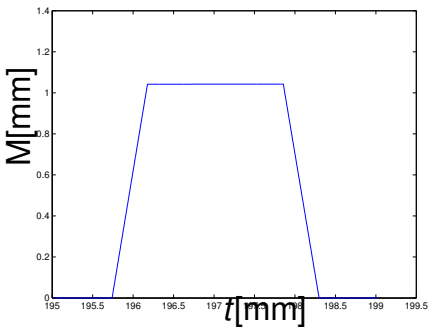

Profiles in *t*

Separable Footprint (SF) Approximation

- Why separable footprint approximation?
  - Inspired by shapes of true footprint functions.
  - 2D convolutions simplify to 1D convolutions.
- $$q(s,t;\beta;\vec{n}) \approx q_{\text{ap}}(s,t;\beta;\vec{n}) \triangleq l(s,t;\beta;\vec{n}) q_{\text{sf}}(s,t;\beta;\vec{n}).$$
  - 2D separable function with unit maximum amplitude

$$q_{\text{sf}}(s,t;\beta;\vec{n}) \triangleq q_1(s;\beta;\vec{n}) q_2(t;\beta;\vec{n}).$$

  - $l(s,t;\beta;\vec{n})$ denotes the "amplitude".

Separable Blurred Footprint

- Assume separable and shift-invariant detector blur:

$$h(s,t) = h_1(s)h_2(t).$$

- (Almost) separable blurred footprint:

$$F_{\mathrm{sf}}(s_k, t_l; \beta; \vec{n}) = \underbrace{l(s_k, t_l; \beta; \vec{n})}_{\text{amplitude}} \underbrace{F_1(s_k; \beta; \vec{n})}_{\text{transaxial}} \underbrace{F_2(t_l; \beta; \vec{n})}_{\text{axial}},$$

where

$$F_1(s_k; \beta; \vec{n}) \triangleq \int h_1(s_k - s) q_1(s; \beta; \vec{n}) \, \mathrm{d}s$$

$$F_2(t_l; \beta; \vec{n}) \triangleq \int h_2(t_l - t) q_2(t; \beta; \vec{n}) \, \mathrm{d}t \, .$$

SF-TR and ST-TT Projector

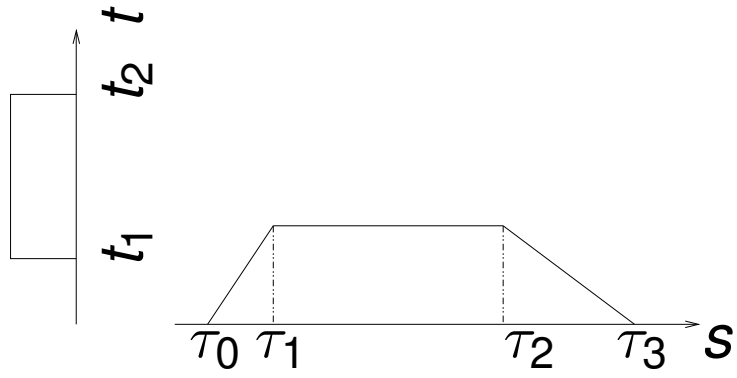

- SF-TR: Trapezoid/Rectangle
  - Trapezoid function in s: $q_1(s;\beta;\vec{n}) \triangleq \mathrm{trap}(s;\tau_0,\tau_1,\tau_2,\tau_3)$
  - Rectangular function in t: $q_2(t;\beta;\vec{n}) \triangleq \mathbb{1}_{\{t_1\le t\le t_2\}}$

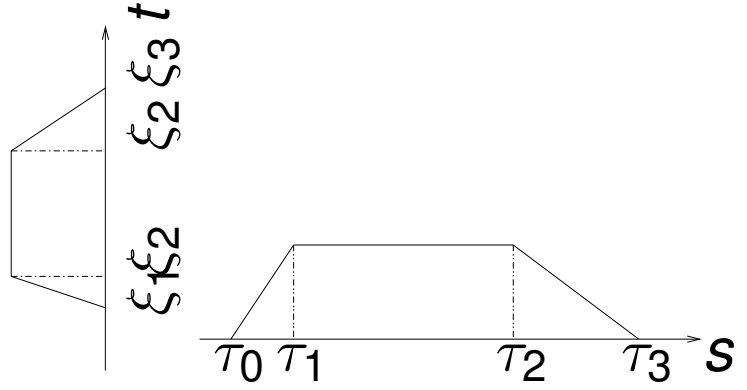

- SF-TT: Trapezoid/Trapezoid
  - Trapezoid function in s: $q_1(s;\beta;\vec{n}) \triangleq \mathrm{trap}(s;\tau_0,\tau_1,\tau_2,\tau_3)$
  - Trapezoid function in t: $q_2(t;\beta;\vec{n}) \triangleq \mathrm{trap}(t;\xi_0,\xi_1,\xi_2,\xi_3)$

SF-TR and ST-TT Projector (cont.)

- Choose vertices of the approximating footprints to match exactly the projections of the voxel boundaries.
  - Approximation adapts to relative positions of source, voxels and detector, as true footprints do.
  - Models depth-dependent magnification accurately.
- SF-TR vs. SF-TT
  - SF-TR is accurate for small cone angle ($< 2^\circ$) geometries, *e.g.*, multi-slice detector geometries.
  - SF-TT is more accurate for large cone angle ($> 10^\circ$) geometries, *e.g.*, flat-panel detector geometries
  - SF-TR is faster than SF-TT.
  - Could be combined to balance computation and accuracy.

Blurred footprint approximations: near $z = 0$

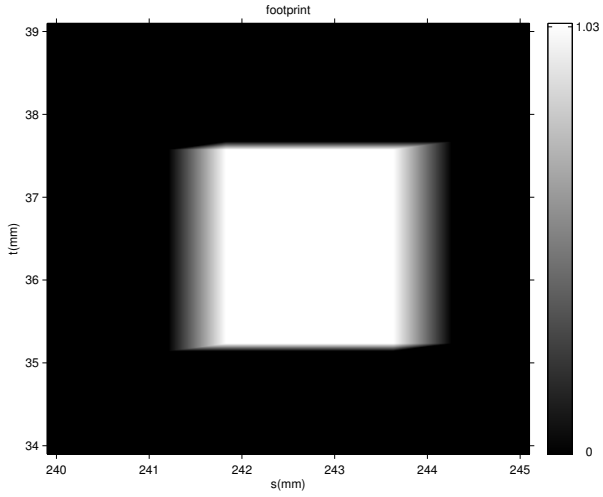

$q(s, t; \beta; \vec{n})$

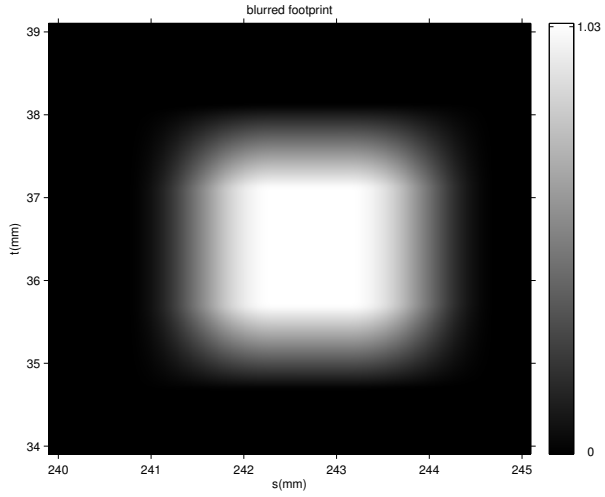

$F(s, t; \beta; \vec{n})$

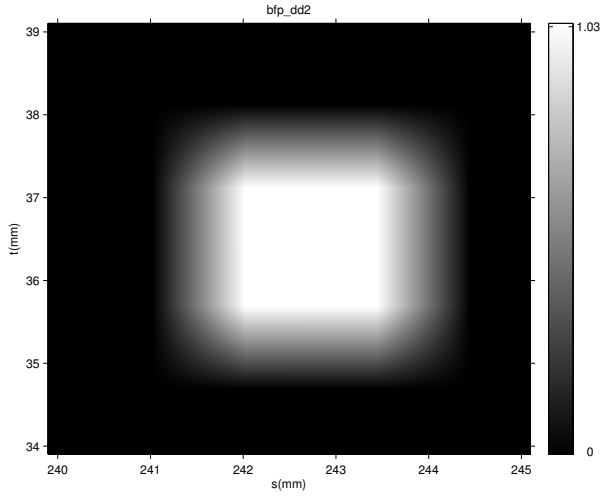

$F_{DD}(s, t; \beta; \vec{n})$

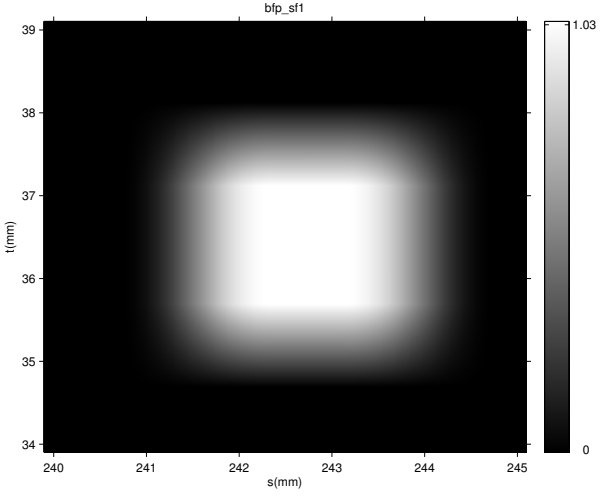

$F_{SF-TR}(s, t; \beta; \vec{n})$

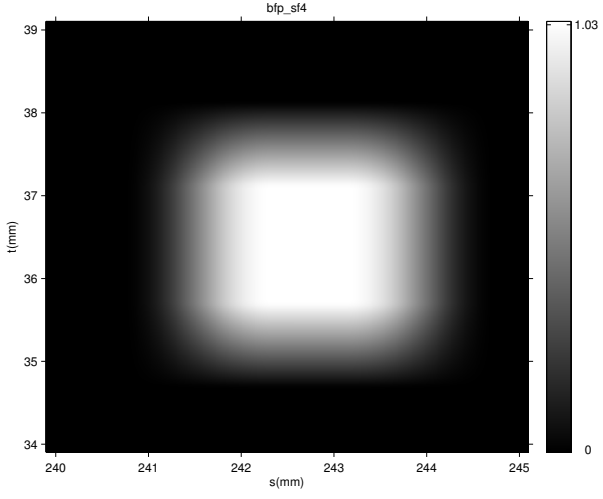

$F_{SF-TT}(s, t; \beta; \vec{n})$

$\vec{n} = (100, 150, 15)$, $\beta = 0$

Azimuthal angle through voxel center: 14.3°. Polar angle: 2.1°.

Blurred footprint approximations: off center

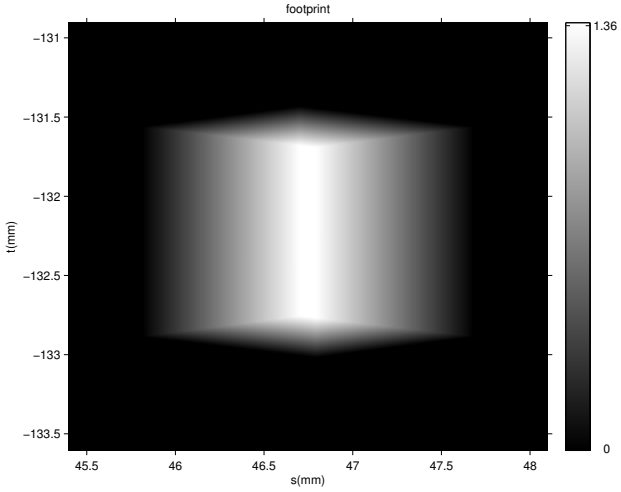

$q(s, t; \beta; \vec{n})$

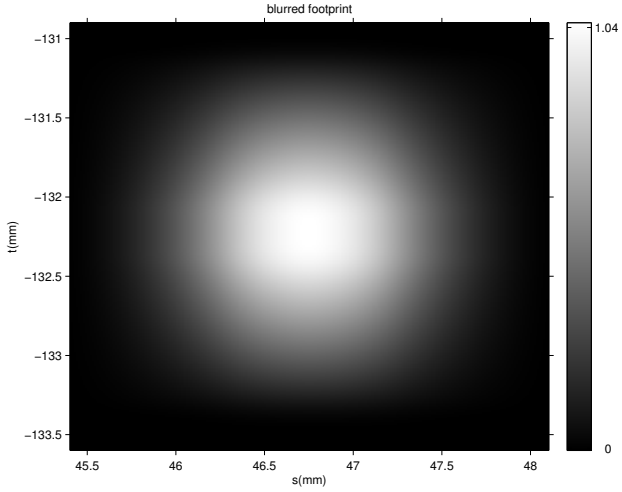

$F(s, t; \beta; \vec{n})$

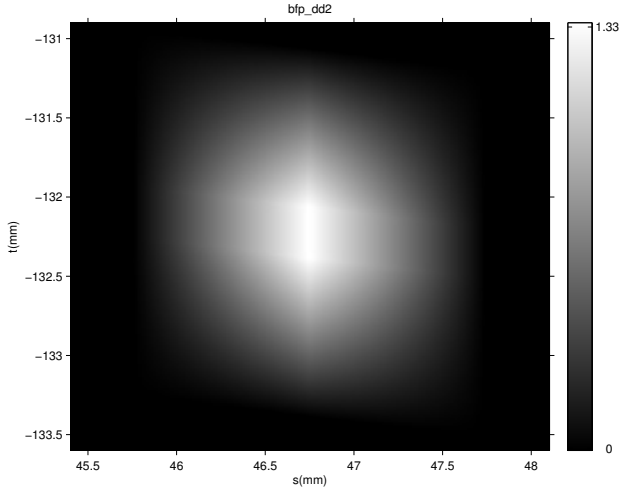

$F_{DD}(s, t; \beta; \vec{n})$

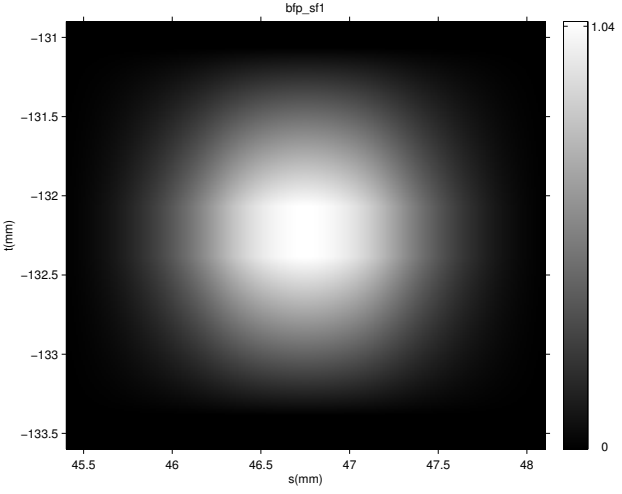

$F_{SF-TR}(s, t; \beta; \vec{n})$

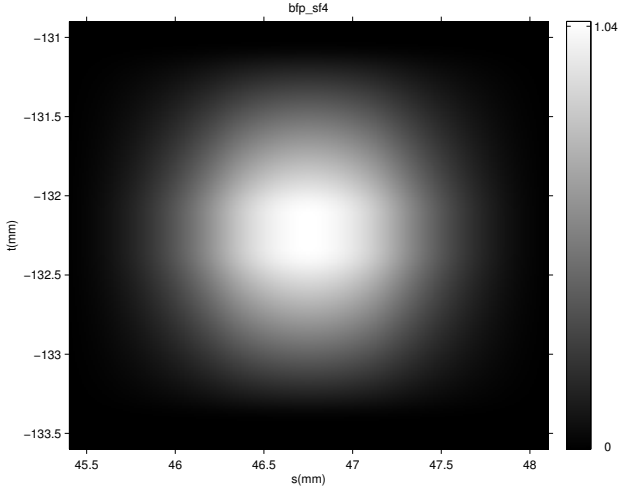

$F_{SF-TT}(s, t; \beta; \vec{n})$

$\vec{n} = (100, 150, -100)$, $\beta = 135°$

Azimuthal angle through voxel center: 138°. Polar angle: 7.8°.

Results: Projector maximum error (single voxel)

Error between exact blurred footprint and an approximation:

$$e(\beta;\vec{n}) \triangleq \max_{s,t\in\mathbb{R}} \left| F(s,t;\beta;\vec{n}) - F_{\text{approximation}}(s,t;\beta;\vec{n}) \right|$$

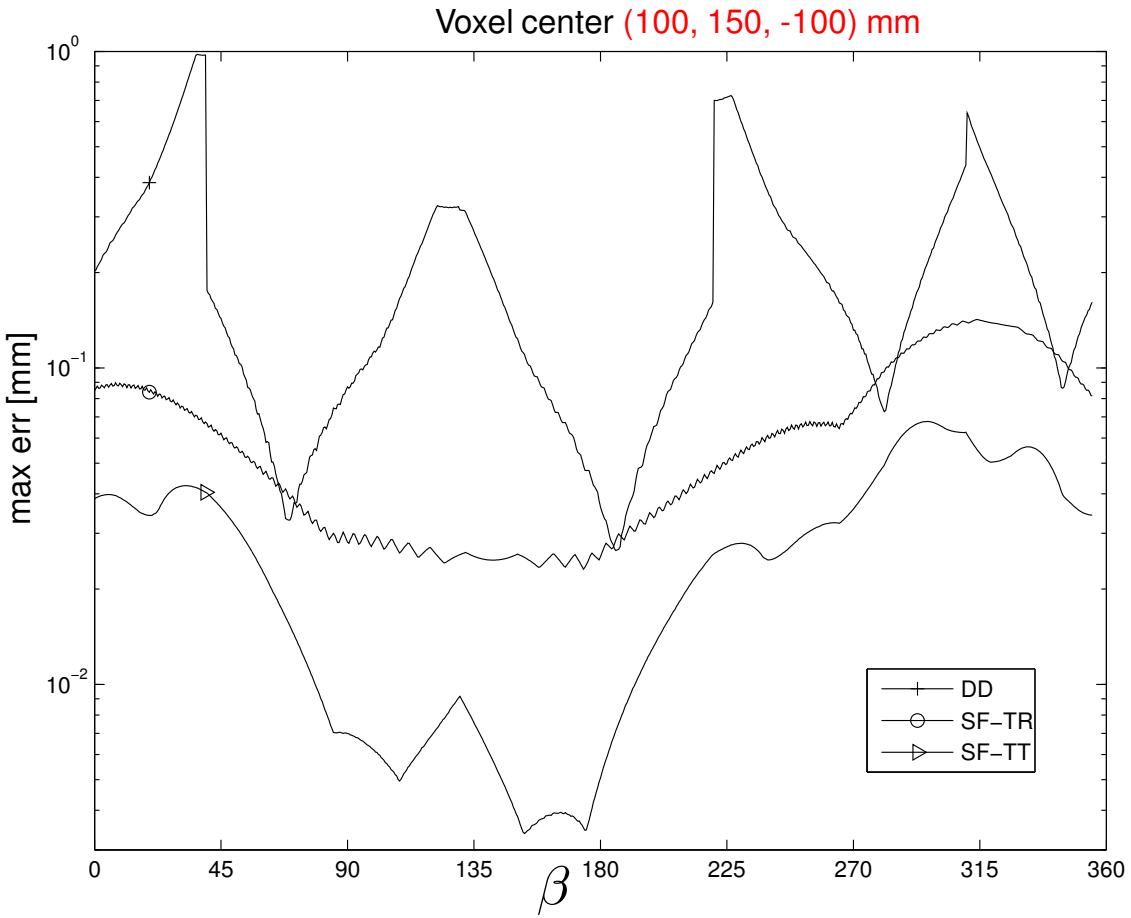

Maximum errors on a logarithmic scale for a 1mm^3 size voxel.

Results: Projector maximum error (single voxel)

For a voxel at origin:

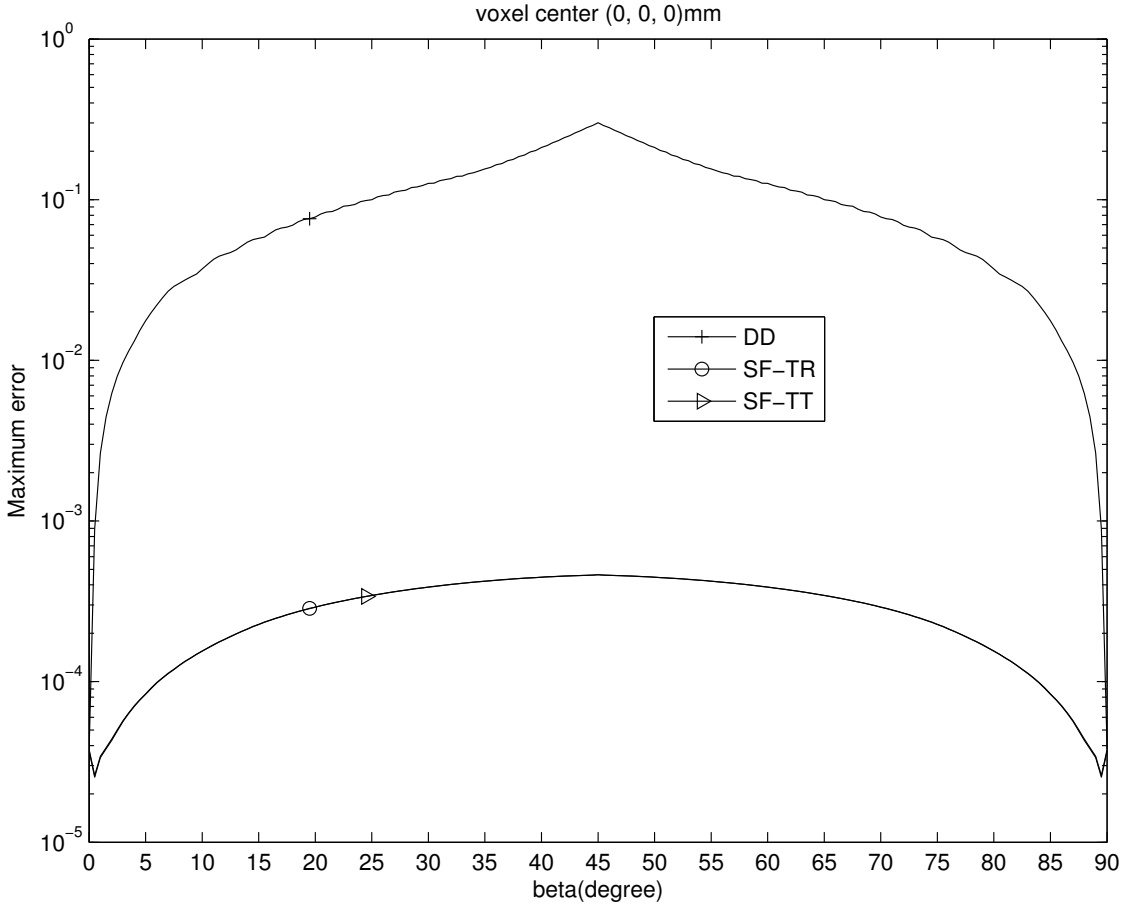

Maximum errors on a logarithmic scale for a 1mm^3 size voxel.

Results: Projector computation time

Projectors	DD	SF-TR	SF-TT
Forward (s)	46	35	91
Back (s)	49	44	92

Forward project a $512 \times 512 \times 128$ image with $\Delta_X = 0.5$ mm.
Back-project a $512 \times 512 \times 984$ sinogram with detector cell spacing of 1 mm.

Elapsed time for 16 POSIX threads, averaged over 5 projector runs.

Iterative full FOV reconstruction: SF-TR vs. DD

SF-TR

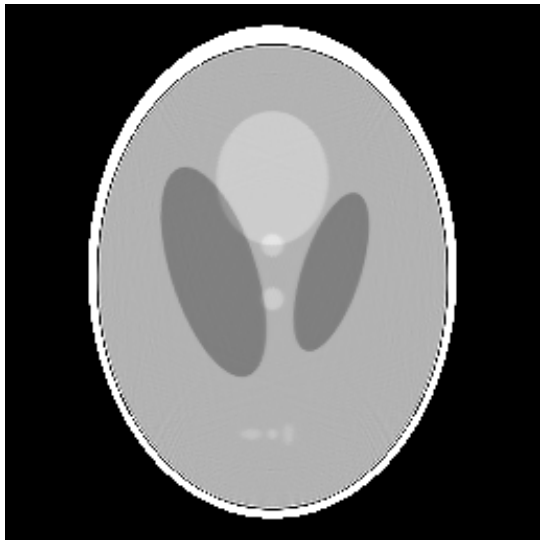

DD

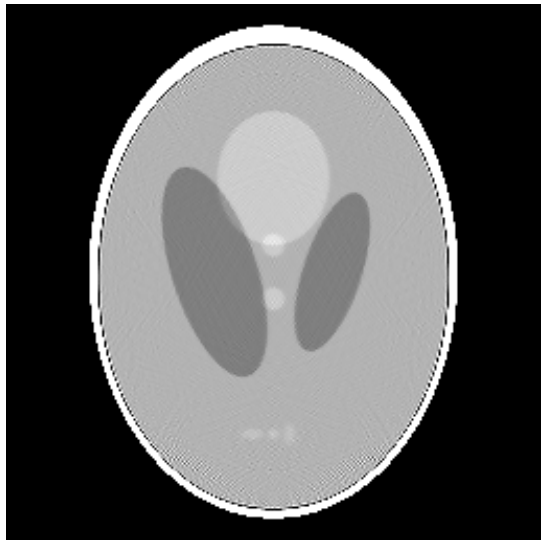

Axial views of reconstructions by PWLS-CG iterative method.
Image size: $256 \times 256 \times 64$ with $\vec{\Delta} = 0.9766 \times 0.9766 \times 0.6250\ \mathrm{mm}^3$.
SF-TT visually indistinguishable from SF-TR for this object and geometry,
as well as for several other geometries investigated, including both axial and helical with flat-panel cone angle $> 10^\circ$.

DD reconstruction (1 mm voxels)

SF-TR reconstruction (1 mm voxels)

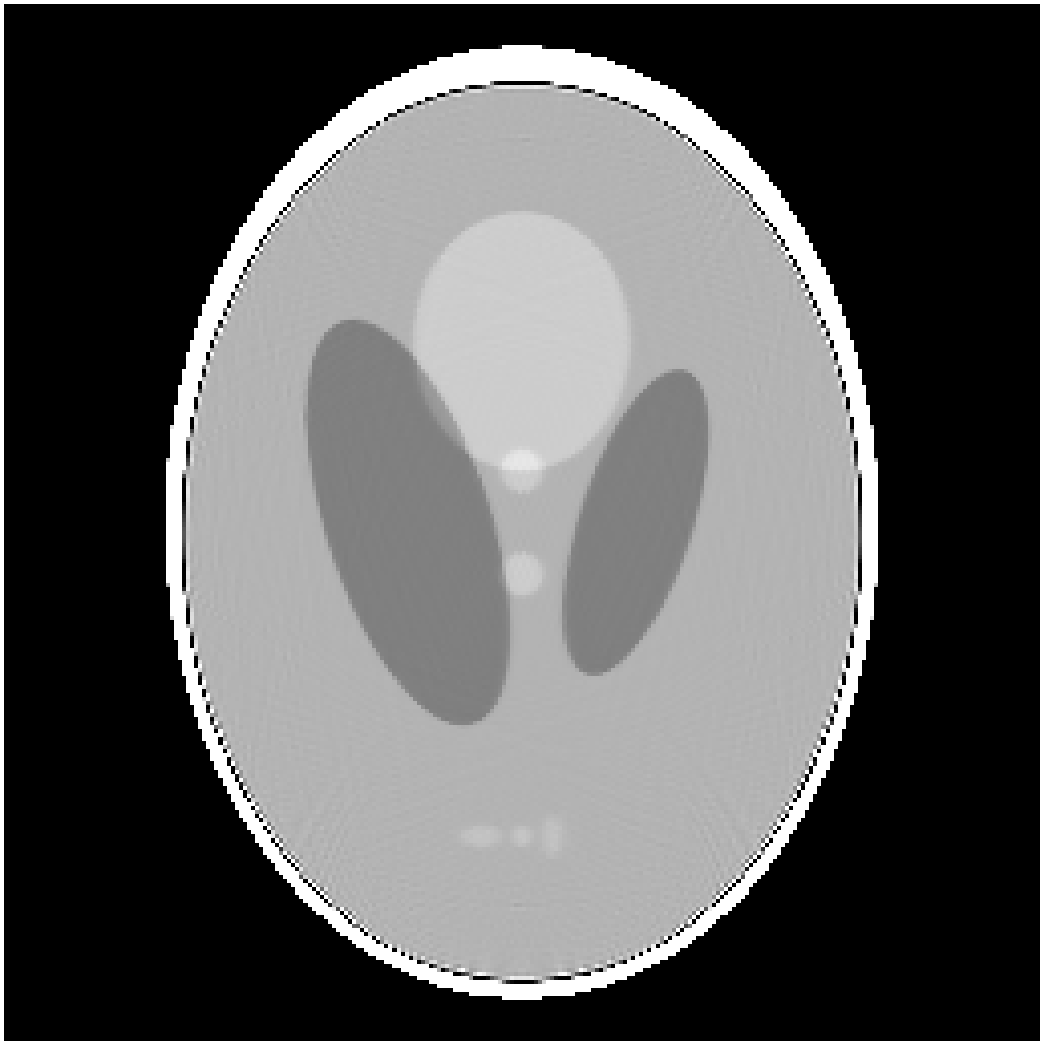

Discussion

- Proposed the SF-TT projector.

Projector	speed	accuracy	cone angle
SF-TR	Fast	High	$< 2^\circ$
SF-TT	Slow	Higher	$> 10^\circ$

- Could combine them to balance computation and accuracy.
- SF-TR adequate for reconstructions under typical CT geometries (no obvious visual differences between SF-TR and SF-TT).